

[†]Cayman Chemical Co., 1180 East Ellsworth, Ann Arbor, MI 48108, USA, [‡]California Institute for Biomedical Research, 11119 North Torrey Pines Road, La Jolla, CA 92037, USA, [§]Department of Molecular and Integrative Physiology, University of Michigan Medical School, Ann Arbor, MI 48109, USA, [¶]Department of Chemistry, The Scripps Research Institute, 10550 North Torrey Pines Road, La Jolla, CA 92037, USA, ^{||}Department of Molecular and Integrative Physiology; Department of Internal Medicine, Division of Gastroenterology; Rogel Cancer Center, University of Michigan, Ann Arbor, MI 48109, USA, [¶]Co-first authors, [¶]To whom correspondence should be addressed: clyssiot@med.umich.edu

Abstract

The objective of this study was to understand and interpret the mechanism of action of a novel inhibitor for glutamate oxaloacetate transaminase 1 (GOT1, also known as aspartate aminotransferase).

Pancreatic ductal adenocarcinoma (PDA) is the most common form of pancreatic cancer. PDA cells are characterized by dysregulated metabolic programs that facilitate growth and resistance to oxidative stress.¹ Among these programs, the metabolic pathway through GOT1 is utilized by PDA to support cellular redox homeostasis.^{2,3} To date, selective small molecule inhibitors of GOT1 that could serve as starting points for the development of new therapies for pancreatic cancer do not exist. Thus, we performed a high-throughput small molecule *in vitro* screen against GOT1. A lead compound (CBR-101) was identified that had metabolic and growth inhibitory activity in pancreatic cancer cells. Next, *in silico* docking analysis was performed to study inhibitor-GOT1 interactions with a CBR-101 analog (L79015) optimized for solubility. The results suggested competitive binding of the inhibitor with the cofactor pyridoxal 5-phosphate (PLP) in the binding site of GOT1. To better understand the binding mode of L79015 to GOT1, a series of mutant GOT1 enzymes were generated that abolished PLP binding.

Together, *in silico* docking, X-ray crystallography, and thermal shift assays using wild-type and mutant enzymes provided insights into the binding mode of L79015. To this end, the CBR-101 drug scaffold as a GOT1 inhibitor may provide a useful starting point to the development of drugs that target redox balance in pancreatic cancer.

Introduction

- Glutamate oxaloacetate transaminase 1 (GOT1) metabolic pathways have been shown to play a key role in pancreatic cancer and making GOT1 a potential therapeutic target for pancreatic ductal adenocarcinoma (PDA).^{2,3}
- CBR-101 was identified as a first lead compound inhibitor for GOT1 (Figure 1 and 2B).⁴
- In silico* docking, X-ray crystallography, and thermal shift assay utilizing wild-type and mutant GOT1 suggested the binding of CBR-101 is a PLP-competitive inhibitor for GOT1.

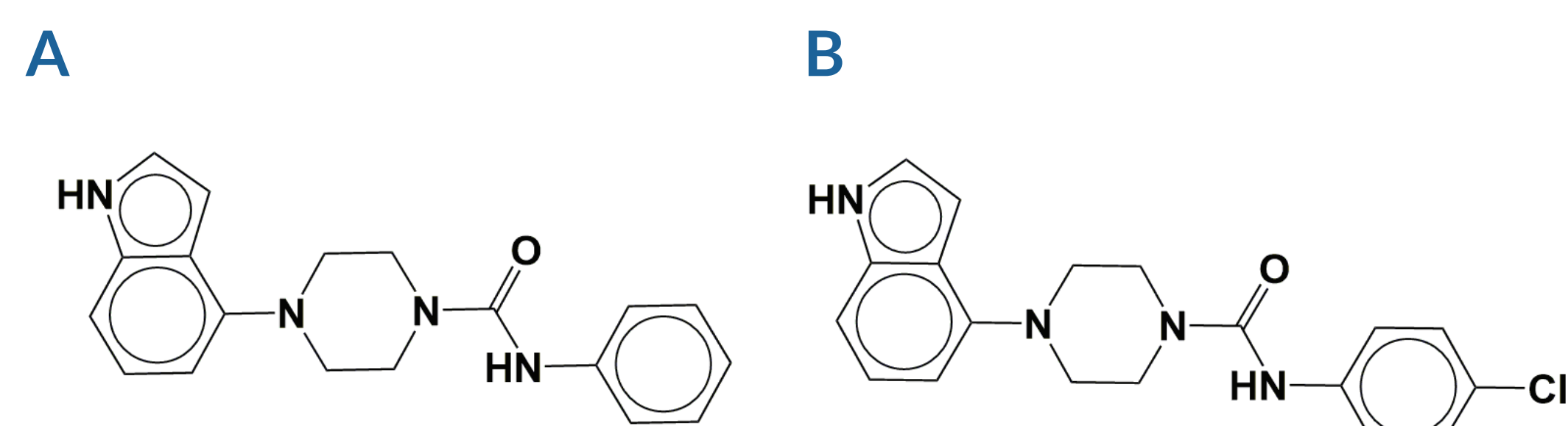


Figure 1 – A. Chemical structure of CBR-101. B. Chemical structure of CBR-101 analog optimized for solubility (L79015).

Methods

Recombinant GOT1 Expression and Purification

All GOT1 proteins (wild-type (WT) and all mutants) were expressed in *E. coli* strain BL21 (DE3) cells. Proteins were purified by immobilized metal affinity chromatography (IMAC) followed by size exclusion chromatography (SEC). For WT-GOT1, dimeric protein was separated from tetrameric protein by SEC, to ensure proteins were monodisperse. Protein was concentrated to 16-38 mg/ml for crystallography.

GOT1/GLOX Specific Activity Assay

Specific activity of GOT1 was measured utilizing two coupling reactions: in the first reaction, 300 ng of WT or mutant GOT1 was coupled with aldehyde oxidase (GLOX) to produce hydrogen peroxide (H₂O₂). For the second reaction and in the presence of horseradish peroxidase (HRP), H₂O₂ oxidizes non-fluorescent Amplex[®] Red producing fluorescent resorufin (Figure 2A).

A linear regression curve relating $\mu\text{Mol H}_2\text{O}_2$ to measured RFU of produced resorufin was generated using Prism (GraphPad). Interpolation using the H₂O₂ standard curve was used to determine $\mu\text{Mol/min/mg}$ velocities for WT or mutant GOT1 (Figure 2C).

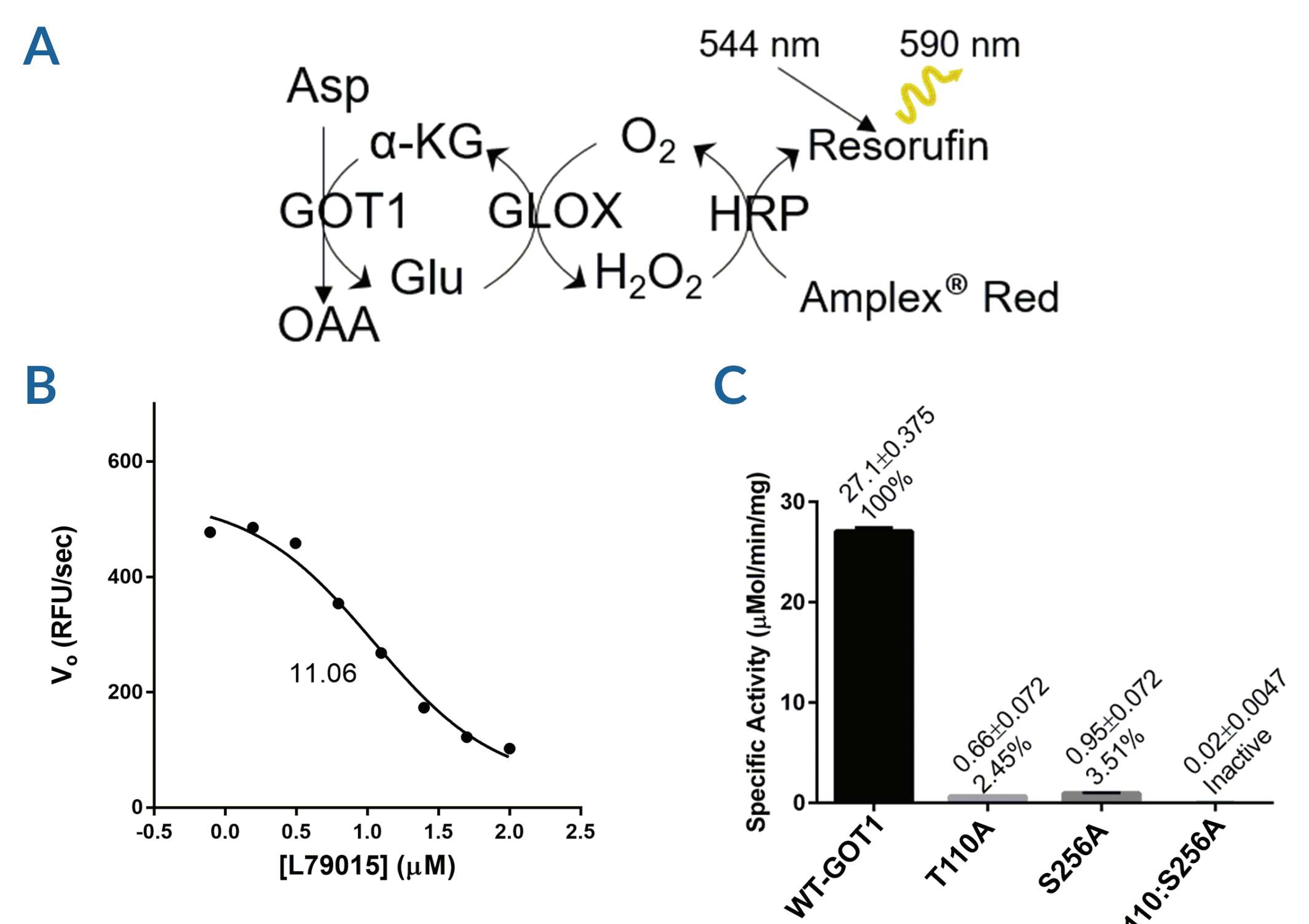


Figure 2 – A. GOT1/GLOX coupled assay. B. Dose-dependent activity of L79015 in the GOT1-GLOX assay; $\text{IC}_{50} = -11.06 \mu\text{M}$. C. Histogram comparing specific activities of WT versus mutant GOT1. The GOT1 double mutant could knock the activity (0.02 $\mu\text{Mol/min/mg}$ versus background detected at 0.04 $\mu\text{Mol/min/mg}$).

In silico Modeling

Glide docking was performed using the WT-GOT1 crystal structure (PDB: 3II0; Figure 3). Model coordinates were prepared for docking using the protein preparation wizard within Maestro 11. Ligands were prepared with LIGPREP from SMILES using an OPLS3 force field modified using EPIK.⁵⁻⁷ A glide grid of 8,000 Å³ was centered on residues previously identified as being near the PLP-binding site including F19, E142, and D223 in the GOT1 crystal structure. Ligand poses were evaluated based on Emodel and Glide scores.

Protein Crystallization and Structure Determination



Figure 3 – GOT1 protein crystals. A. Crystals of WT-GOT1 were grown in 25% (w/v) polyethylene glycol 3,350 and 0.1 M sodium acetate trihydrate, pH 4.5, 5% Cymal. B. Crystals of T110A mutant were grown in 25% (w/v) polyethylene glycol 3,350 and 0.1 M HEPES, pH 7.5. C. Crystals of T110A:S256A mutant were grown in 20% (w/v) polyethylene glycol monomethyl ether 2,000, 0.1 M Tris, pH 8.5, and 0.2 M trimethylamine N-oxide dihydrate. In order to obtain an L79015-bound structure, all crystals were soaked with L79015 in several concentrations (0.15-0.3 mM) over the course of several days and analyzed for diffraction. Diffraction data was collected using LS-CAT sector 21 at APS (advanced photon source). Datasets were processed using HKL-2000 software suite⁸ and structures were solved and refined using MOLREP, COOT, and REFMAC5.⁹ No density was observed for L79015 compound.

Thermal Shift Assays

Thermal shift assays (TSA) were utilized to biophysically characterize each GOT1 mutant in the presence and absence of L79015. GOT1 proteins at 1 mg/ml were mixed 100:1 with Sypro[™] Orange dye. Samples were processed using a Bio-Rad CFX C100 Touch[™] qPCR and the FRET assay settings with a heating ramp of 0.3°C/sec cycling from 4°C to 100°C. Analysis was performed using the Bio-Rad CFX manager software.

Results

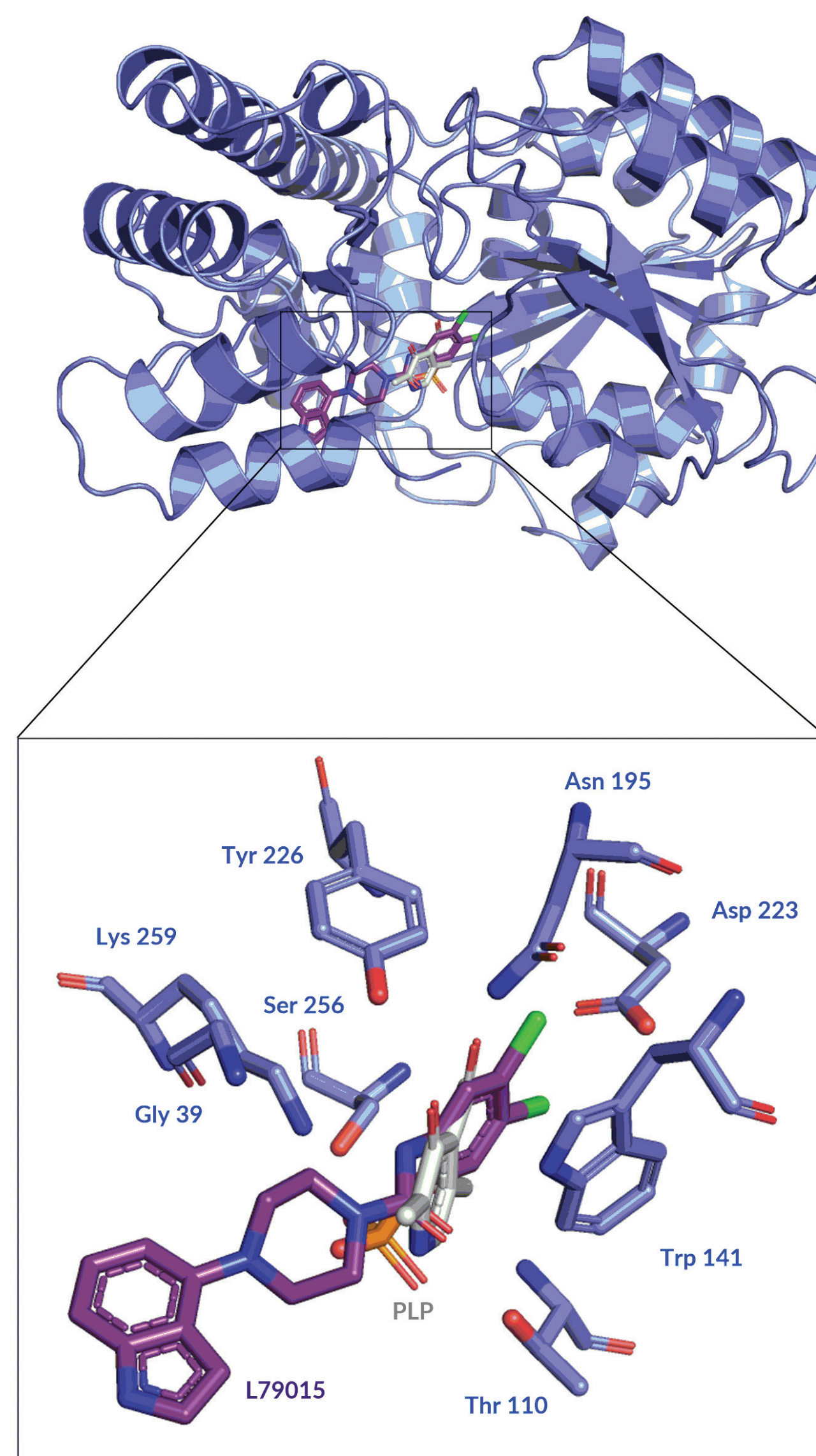


Figure 4 – Overlay of docked WT-GOT1 structure with L79015 (purple, shown in sticks) and PLP (grey, shown in sticks) in the active site. The presented pose showed highest score (-9.6 kcal/mol versus -8.1 kcal/mol for PLP). Thr110 and Ser256 interact with PLP but are not predicted to interact with compound.

For computational analysis, structural biology, and biophysical characterization, a CBR-101 analog (L79015) with increased solubility was utilized (Figure 1B). Docking studies suggested a PLP-competitive binding mode for L79015 (Figure 4). Therefore, a series of mutants were designed and analyzed (T110A, S256A, and T110A:S256A) with the goal of abolishing PLP binding and opening the active site for inhibitor binding. Consequently, single mutants appeared to retain partial activity, although the affinity for PLP was reduced substantially (Figure 2C). T110A:S256A double mutant was completely inactive (Figure 2C). We could successfully obtain crystal structures of native, T110A, and T110A:S256A mutants of GOT1. WT and T110A structures revealed full and partial bound-PLP in their active sites (Figure 5A, 5B, and 5C). T110A:S256A structure showed no PLP bound in the active site as expected (Figure 5D). Comparison of mutant structures to WT revealed a shift near the C-terminal helix (371-411), which is at the dimer interface of tetrameric WT (Figure 6).

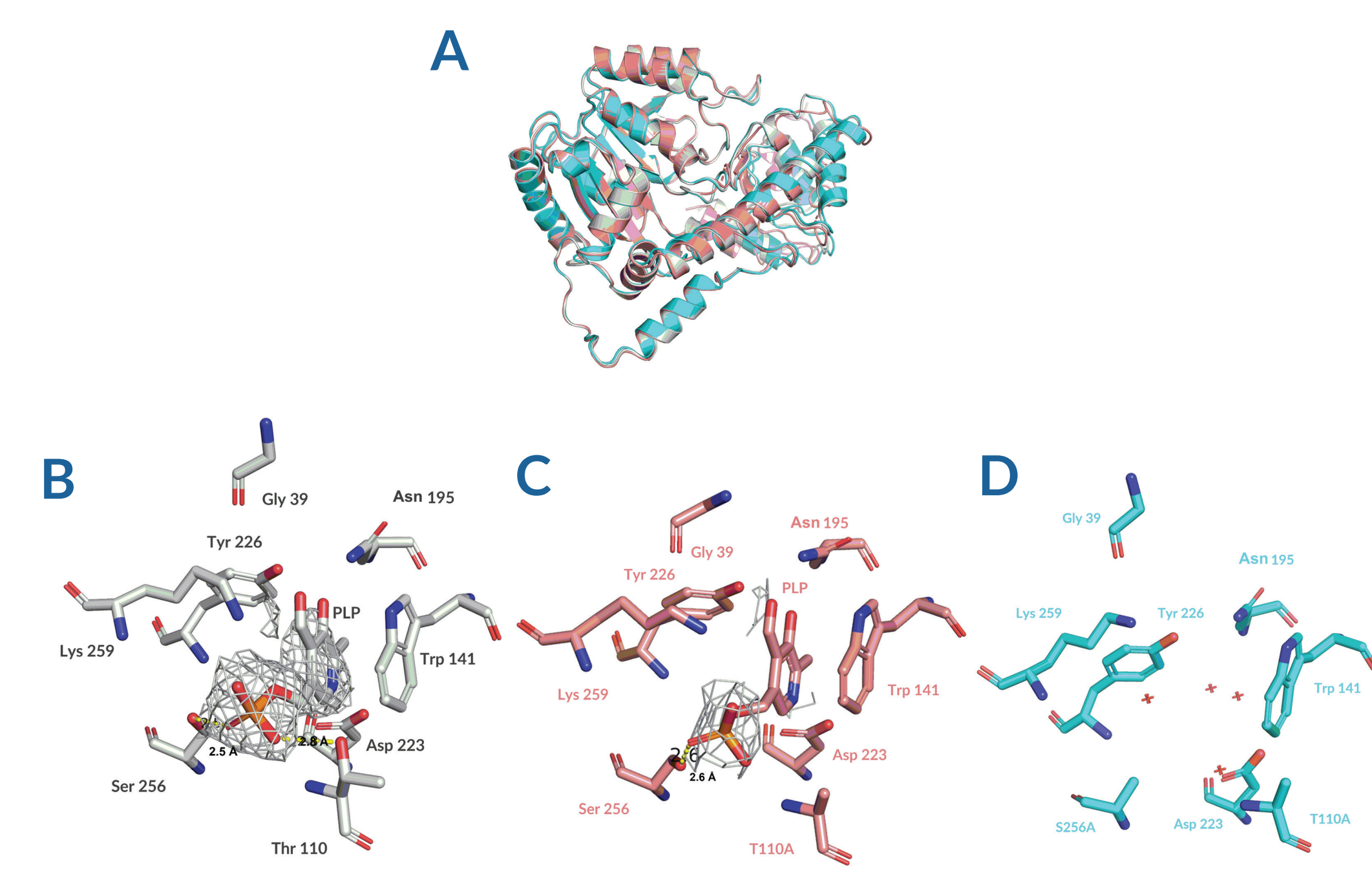


Figure 5 – A. Overlay of WT (grey), T110A (salmon), and T110A:S256A (cyan) GOT1 crystal structures. B. The 2F_o-F_c electron density map (grey) contoured at 1 σ around PLP in WT-GOT1 structure. Hydrogen-bonded distance is shown between Ser256 and PLP. C. The 2F_o-F_c electron density map (grey) contoured at 1 σ around PLP in the T110A mutant structure. D. No density was observed for PLP cofactor in T110A:S256A mutant structure. Residues around PLP site are shown in sticks. Water molecules (red dots) were observed in the PLP site.

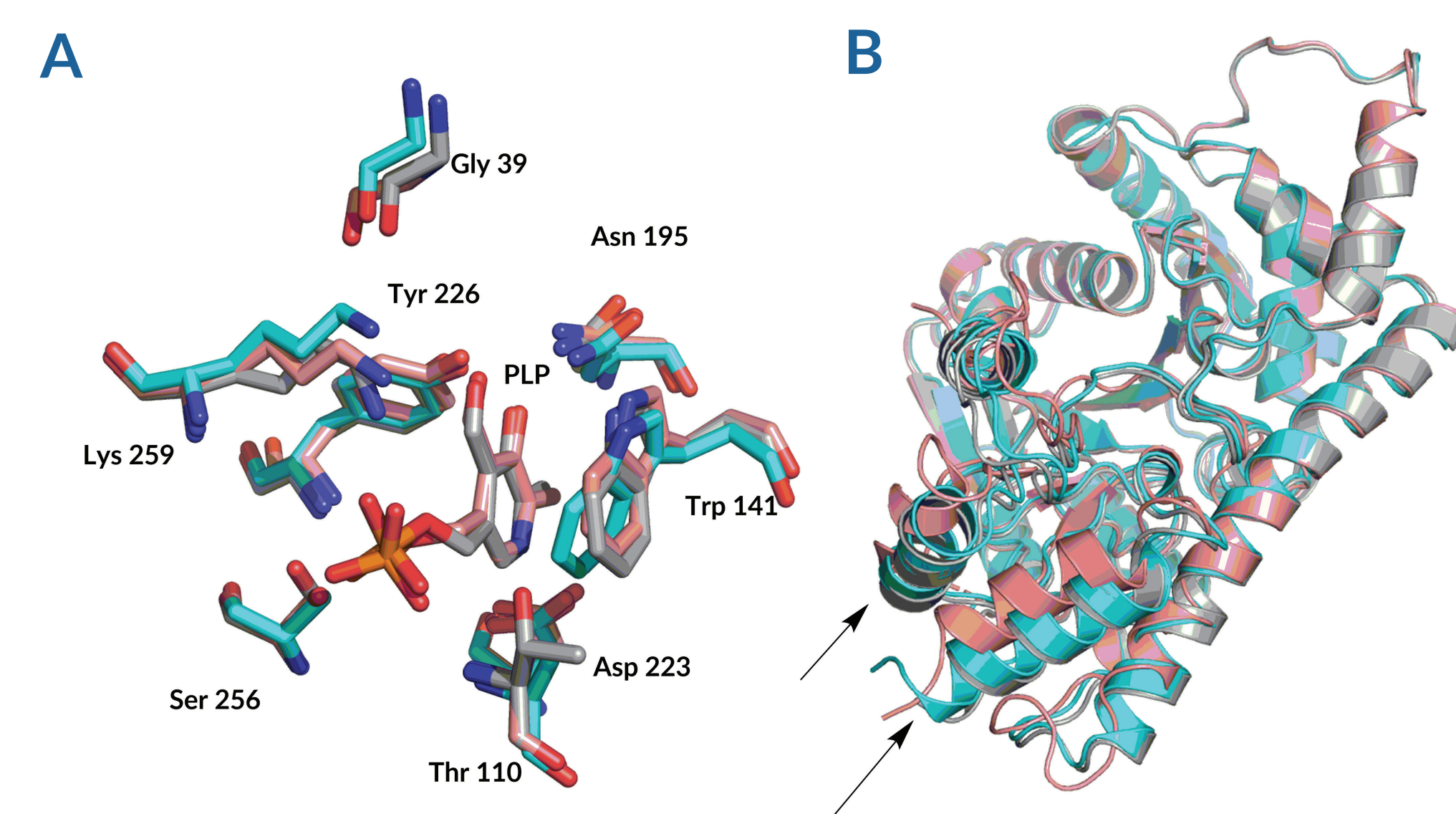


Figure 6 – A. Overlay of the GOT1 binding pocket between WT (grey), T110A (salmon), and T110A:S256A (cyan). B. Overlay of tertiary structures for all three proteins (WT in grey, T110A in salmon, and T110A:S256A in cyan) reveals a translocation in two C-terminus helices.

Based on the TSA result, melting profile near 70°C of WT and single mutants likely corresponds to PLP-bound GOT1 (Figure 7A), while T110A:S256A mutant, shown by crystallography to not bind PLP, displayed a single melting peak at 41.5°C, allowing for the assignment of this peak as the PLP-unbound GOT1 (Figure 7A and 7C). Increasing concentrations of L79015 increased the peak intensity for the unbound state at 40°C (Figure 7B-F). However, it could not fully displace PLP, as the bound form is still observed, suggesting this binding mode is likely transient or weak.

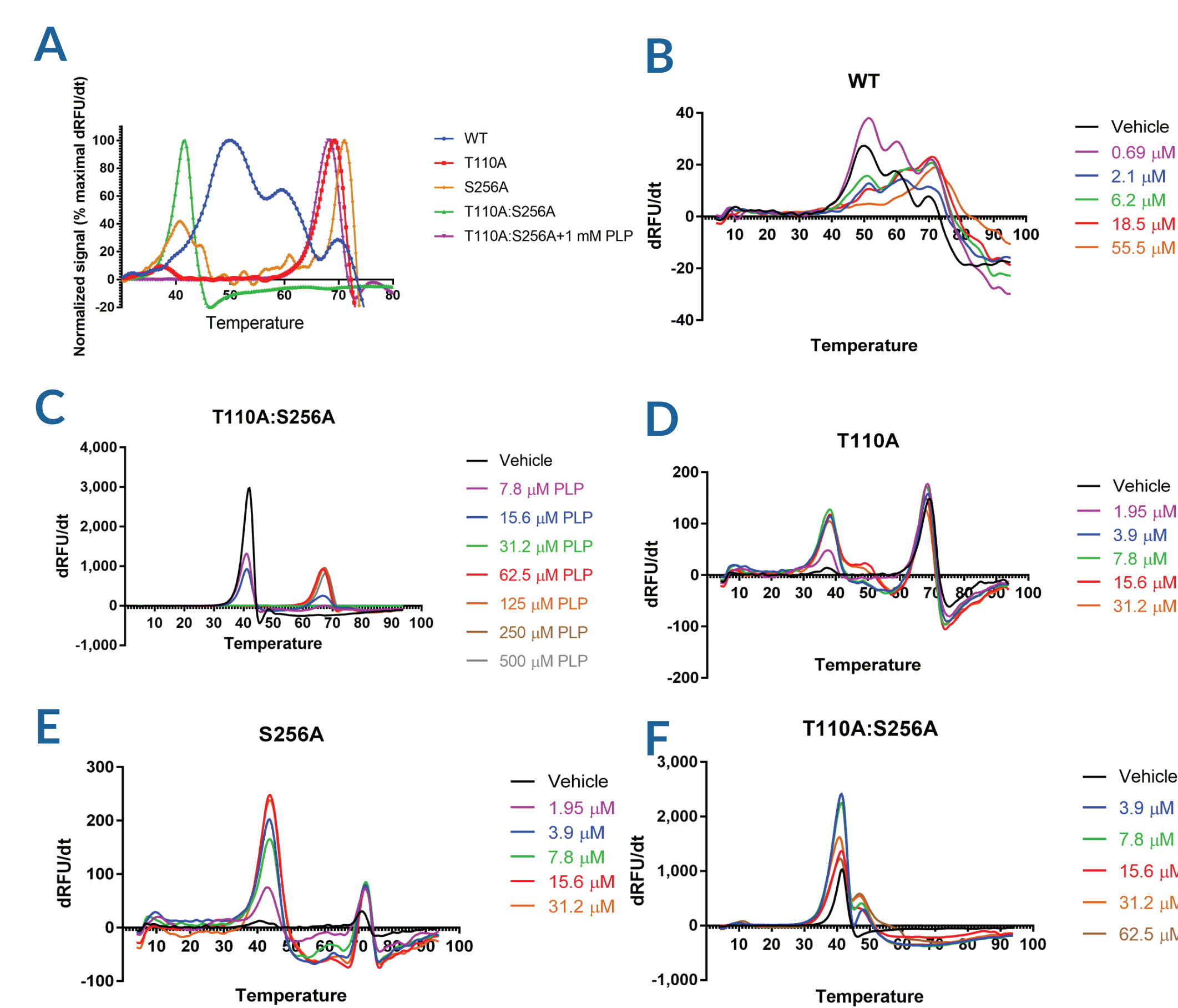


Figure 7 – A. Melting profiles for all mutants. B. Melting profile for L79015-WT titration. C. Melting profile for L79015-T110A titration. D. Melting profile for L79015-T110A titration. E. Melting profile for L79015-S256A titration. F. Melting profile for L79015-T110A:S256A titration.

Conclusions

- Our results support L79015 inhibitor binding through direct competition for the active site in GOT1.
- Mutational studies revealed the relationship between PLP binding and thermal stability of GOT1.
- Also, PLP binding can be disrupted in active site by disturbing the hydrogen bond network within the phosphate group, either partially or entirely, resulting in reduced or ablated GOT1 enzymatic activity.
- Overall, these results provide insight into the mechanism of action for L79015.

References

- Haltiwacker, C.J. and Lyssiotis, C.A. Employing metabolism to improve the diagnosis and treatment of pancreatic cancer. *Cancer Cell* 31(1): 5-19 (2017).
- Yang, C.-S., Stampoulidou, E., Kingston, N.M., et al. Glutamine-utilizing transaminases are a metabolic vulnerability of TAZ/YAP-activated cancer cells. *EMBO Rep.* 19(6): e43577 (2018).
- Gaglio, D., Metello, C.M., Carneiro, P.A., et al. Oncogenic K-Ras decouples glucose and glutamine metabolism to support cancer cell growth. *Mol. Syst. Biol.* 7: 523 (2011).
- Anglin, J., Zawert, R.B., Sanders, P.M., et al. Discovery and optimization of aspartate aminotransferase 1 inhibitors to target redox balance in pancreatic ductal adenocarcinoma. *Bioorg. Med. Chem. Lett.* (2018).
- Greenwood, J.R., Collins, D., Sullivan, A.P., et al. Towards the comprehensive, rapid, and accurate prediction of the favorable tautomeric states of drug-like molecules in aqueous solution. *J. Comput. Aided Mol. Des.* 24(6-7): 591-604 (2010).
- Shelley, J.C., Chollet, A., Frye, L.L., et al. EpiK: A software program for pK_a prediction and protonation state generation for drug-like molecules. *J. Comput. Aided Mol. Des.* 21(12): 681-691 (2007).
- Sastry, G.M., Adzhigey, M., Day, T., et al. Protein and ligand preparation: Parameters, protocols, and influence on virtual screening enrichments. *J. Comput. Aided Mol. Des.* 27(8): 221-234 (2013).
- Wink, M.D., Ballard, C.C., Cowart, K.D., et al. Overview of the CCP4 suite and current developments. *Acta Crystallogr. D* 64(4): 235-242 (2008).
- Vagin, A. and Teplovskoy, A. MOLREP: An automated program for molecular replacement. *J. Appl. Cryst.* 30(6): 1022-1025 (1997).
- Emley, P. Tools for ligand validation in Coot. *Acta Crystallogr. D* 59(1): 203-210 (2003).
- Murshudov, G.N., Skubnik, P., Lebedev, A.A., et al. REFMAC5: The refinement of macromolecular crystal structures. *Acta Crystallogr. D* 67(Pt 4): 355-367 (2011).